Contreras-García, J.; Izquierdo-Ruiz, F.; Marqués, M.; Manjón, F. (2020). Borates or phosphates? That is the question. Acta Crystallographica Section A: Foundations and Advances. 76:197-205. https://doi.org/10.1107/S2053273319016826

Borates or phosphates? This is the question

J. Contreras-García,[a*] F. Izquierdo-Ruiz,[b] M. Marqués[c] and F.J. Manjón[d*]

[a] *Laboratoire de Chimie Théorique, UPMC, Sorbonne Universités and CNRS, Paris 75005 (France)*

[b] *Departamento de Química Física y Analítica, MALTA-Consolider Team, Universidad de Oviedo, Oviedo E-33006 (Spain)*

[c] *Centre for Science at Extreme Conditions and School of Physics and Astronomy, and, The University of Edinburgh, Edinburgh, EH9 3FD (UK)*

[d] *Instituto de Diseño para la Fabricación y Producción Automatizada, MALTA-Consolider Team, Universitat Politècnica de València, Valencia 46022 (Spain)*

Synopsis - A new nomenclature is proposed for borates from quantum chemistry grounds that is in agreement with their properties and recovers the predictive power of Fukunada and Yamaoka phase transition diagram.

Abstract - Chemical nomenclature is perceived to be a closed topic. However, this work shows that the identification of polyanionic groups is still ambiguous and so is the nomenclature for some ternary compounds. Two examples, boron phosphate (BPO_4) and boron arsenate ($BAsO_4$), which were assigned to the large phosphate and arsenate families, respectively, nearly a century ago, are explored. The analyses show that these two compounds should be renamed phosphorus borate (PBO_4) and arsenic borate ($AsBO_4$). Beyond epistemology, this has pleasing consequences at several levels for the predictive character of chemistry. It paves the way for future work on the possible synthesis of $SbBO_4$ and $BiBO_4$, and it also renders previous structure field maps completely predictive, allowing us to foresee the structure and phase transitions of $NbBO_4$ and $TaBO_4$. Overall, this work demonstrates that quantum mechanics calculations can contribute to the improvement of current chemical nomenclature. Such revisitation is necessary to classify compounds and understand their properties, leading to the main final aim of a chemist: predicting new compounds, their structures, and their transformations.

Keywords: - borates; topology; electron density; nomenclature

1. Framework

The part of chemical nomenclature related to the systematic classification of compounds, as introduced by Pauling nearly a century ago, is perceived to be a rather closed topic (1). In particular, the notation of ternary polycationic ABX_n compounds (*A* and *B* cations and *X* anion) was assumed to be that of pseudo-binary *AX* compounds by noting them as one cation - *A*, and one anion - BX_n. Under this notation, ABX_n compounds can be understood as the composition of polyhedral units, formed by *X* anions around *A* (AX_o) and *B* (BX_m) cations. The polyanionic group BX_m is usually formed by cation *B* with higher valence and smaller coordination, which, according to Pauling's rules, has the stronger electrostatic bond with anion *X*. In this way, BX_m groups form closed units that tend to separate highly charged *B* cations amongst them, so as to reduce the electrostatic repulsion between these cations (e.g. cyanates or phosphates) (2).

The rules for naming inorganic compounds were revised in 1970 (3), when a non-ambiguous notation was favoured over chemical insight. As an example, in the classical nomenclature, phosphate represented polyanion PO_4^{3-}, whereas phosphite referred to PO_3^{3-}. Within the 1970 IUPAC rules, phosphate defines a general negative group with phosphorous as the central atom, irrespective of the oxidation state. However, the existence/recognition of such polyatomic units in complex compounds, without resorting to chemical intuition, may lead to ambiguous cases. Here, we aim at illustrating one of these cases, by analysing in particular ABO_4 compounds containing boron. The natural question lies in how to determine which of the cations should be labelled "*A"* and which "*B"*, i.e., which one is the main polyatomic anion. For clarity, general *B* cations will be noted in italic, *B*, whereas the boron atom will be noted in regular capital B. Historically, several criteria have been proposed to identify these *B* cations: structural similarity, polyhedral compressibility, valence, and size to cite the most important ones. In most ABO_4 compounds with a quartz-related structure (i.e., composed by AO_4 and BO_4 tetrahedra), all the above mentioned criteria converge. Here we will show that this is not the case for the boron-containing compounds.

Understanding the ambient and pressure-induced phases of ABO_4 compounds, as well as their behaviour under compression, is a challenging task within Crystal Chemistry, with implications extending to many fields, including earth, planetary, and material sciences. Furthermore, since many properties of materials, such as piezoelectricity or thermal expansion, depend on the crystalline structure, it becomes imperative to predict the different phases of materials for technological applications (4). A well-known example, due to its relevance in earth sciences and in different technologies, like radiative waste recovery, is the family of orthosilicates that includes the minerals zircon ($ZrSiO_4$) and hafnon ($HfSiO_4$). Many orthosilicates crystallize in the zircon-type structure and undergo a pressure-induced phase transition to the scheelite-type structure. Curiously enough, these compounds can be recovered in the metastable scheelite phase at room pressure since they do not revert to the original zircon-type phase upon decompression; thus leading to improved properties for certain applications with respect to the original zircon-type phase (5; 6).

Predicting the structure of a solid of a given composition at a determined temperature and pressure is of the uttermost importance in Solid State Science. Until the recent advent of metadynamics and genetic algorithms, the task of predicting the structure of a solid compound was accomplished through trial-and-error. The consequent use of structure field maps or diagrams was a step in the right design direction. These maps enable predicting the structure of a given compound based on ionic parameters (typically ionic radii). Given the current computational price of predictive algorithms, these maps still play a major role in the structure prediction of a compound given its composition, both at ambient conditions and at extreme temperature-pressure conditions. Hence, general classifications of compounds in structure field maps or diagrams are crucial when it comes to predicting crystalline structure and phase transformations under pressure (i.e. their "reactivity") (7).

In particular, it is possible to find general trends of ABO_4 compounds in terms of the properties of *A* and *B* cations that enable the prediction of the room pressure structure for a given compound, and its transformations under pressure. In this context, diagrams of ABO_4

compounds have been usually constructed assuming pseudo-binary compounds, formed by A^{x+} and $(BO_m)^{x-}$ ions, where the BO_m group is the polyatomic anion that gives name to the compound (e.g. silicate, phosphate). Once the polyanion is known, the classification is usually done in terms of ionic radii (8; 9; 10; 11; 12; 13; 14). Therefore, the identification of the main polyanion is critical to classifying the structural behaviour of ABO_4 compounds and circumventing extensive (and expensive) calculations.

The diagrams for ABO_4 compounds are very rich. Indeed, the large number of cations whose valence sum up to +8 leads to many $A^xB^{8-x}O_4$ combinations, so the ABO_4 family is large and diverse. In order to simplify its characterization, ABO_4 compounds are divided into subfamilies based on the forming polyanion (15) (see **S.I.** for a brief enumeration). Among these subfamilies (15), the shortest and less recognized one (by far) is the orthoborate (BO_4) family, whose only known members to date are the very rare minerals of schiavinatoite ($NbBO_4$) and behierite ($TaBO_4$), crystallizing in the zircon-type structure (16; 17; 18; 19; 20; 21), as well as possibly VBO_4, merely referred to as BVO_4 in Ref. (7). Contrary to expectation, this last compound was not found to be isostructural to silica, and no data has been found about its precise structure (19). Overall, the orthoborate family of ABO_4 compounds is so poorly understood that the compound $TaBO_4$ was named as $BTaO_4$ in Ref. (11), despite it crystallizes in the zircon-type structure (no tantalate is known to crystallize in the zircon-type structure!) and that it was named as tantalum borate in a previous work (22). In this context, the omission of the orthoborate subfamily in the first reviews on the systematization of ABX_4 crystal structures and their transformations (11; 12) is not surprising.

Apart from the schiavinatoite and behierite minerals, and the brief mention of BVO_4, there are two other boron-containing ABO_4 compounds, which have also been known for more than a century (23): boron phosphate (BPO_4) and boron arsenate ($BAsO_4$), both crystallizing in the high cristoballite (*I*-4, No. 82, Z=4) structure (24). This structure can be viewed as formed by PO_4 (AsO_4) and BO_4 polyhedra, which are linked by their corners (**Figure 1**). Following Pauling's rules, they were respectively named boron phosphate and boron arsenate more than a century ago, due to the larger valence of P and As (5+), as opposed to that of B (3+). In other words, PO_4 and AsO_4 were assumed to be the main polyatomic units. The nomenclature choice was also supported by the structure. Both compounds crystallize in the high-cristobalite structure, which derives from the α-quartz structure, comparable to the berlinite structure of aluminium phosphate ($AlPO_4$) and aluminium arsenate ($AlAsO_4$) (25; 26).

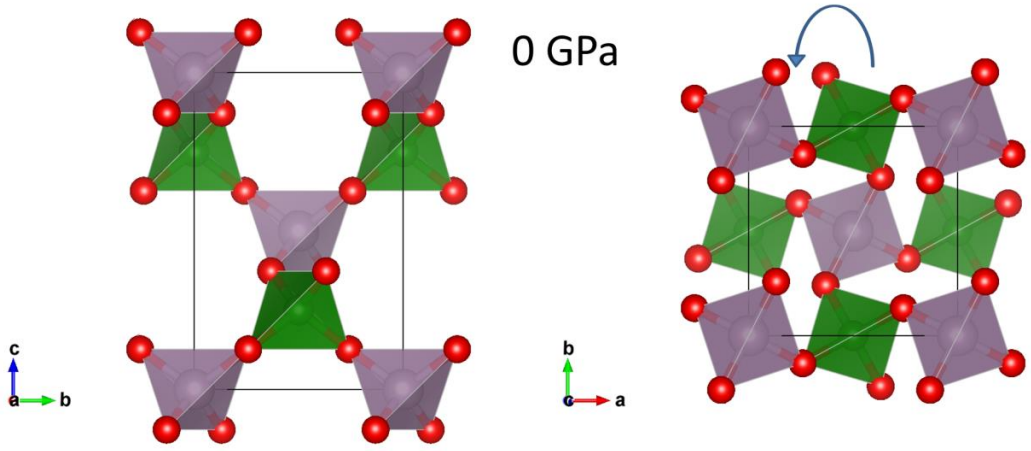

Figure 1. Polyhedral image of PBO_4 at ambient pressure across the *bc* and *ab* planes. PO_4 polyhedra are depicted in green and BO_4 polyhedra in purple.

Building upon the previous reasoning, the classical nomenclature was also supported by the traditional polyhedral compressibility approach in Solid State Science. The compressibility of ABO_4 compounds has been usually summarized in terms of the compressibility of polyhedral units around *A* and *B* cations (27). It suffices to identify the *A*

cation as the one that leads to the most compressible polyatomic AO_o unit. In this way, the polyhedron AO_o governs the compressibility of the material, while the BO_m unit is the "fixed" or incompressible polyanion (28). When this approach is used for BPO_4 and $BAsO_4$, PO_4 comes out as the natural main unit in BPO_4, whereas this is doubtful in the case of $BAsO_4$ (see **Figure S1**).

All in all, the historical classification of BPO_4 and $BAsO_4$ is substantially supported from all classical pointers except one. The pressure-induced phase transitions observed in these compounds do not match those observed in related phosphates and arsenates, such as $AlPO_4$ and $AlAsO_4$. In this context, Fukunaga and Yamaoka's (FY's) diagram (11) provides an extensive rationalization of the ambient phase and pressure-induced phase transitions in ABO_4 compounds (**Figure 2**). This diagram is organized in terms of two variables: $t=(r_A+r_B)/2r_O$ in the abscissa and $k=r_A/r_B$ in the ordinate, where r_A, r_B, and r_O are the ionic radii of the A and B cations, and oxygen, respectively. This diagram enables the prediction of the structure of a given ABO_4 compound at ambient conditions with good accuracy. Moreover, a "south-east" rule is observed upon pressurization (t increases, k decreases), which enables the prediction of structural transformations under pressure assuming that pressure leads to: i) a greater compression of the oxygen anion over that of the cations, and ii) a greater compression of cation A over that of cation B. In FY's diagram, the Pauling's valence rule is used to decide on the main unit, so that A cations should have the smaller valence. Since we are comparing boron (3+) with pnictogen atoms (5+), the traditional assignment is again supported.

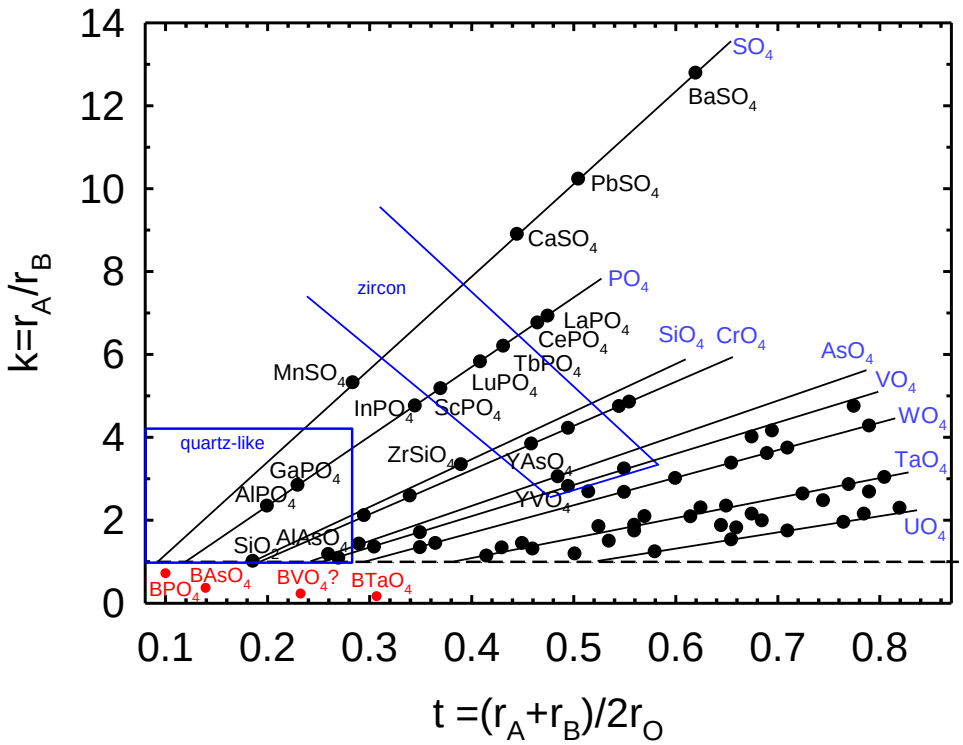

Figure 2. Original FY's diagram with BPO_4, $BAsO_4$ and other boron-related compounds (in red color) as if they were $A^{3+}B^{5+}O_4$ compounds where A is boron, hence with k<1. Clearly, the formulation $BTaO_4$ is not compatible with the observed zircon structure at room conditions.

However, this attribution challenges the predictive power of FY's diagram, which for the first time does not hold neither for BPO_4 nor for $BAsO_4$. These two compounds undergo a transition at high pressure and high temperature from the high cristobalite (29) to the berlinite (or low quartz) structure (**Figure 2)** (30), i.e. they follow an anomalous "north-east" behavior in FY's diagram. It must be stressed that such anomaly would also affect $BTaO_4$, which was

already known to be a zircon-type compound (7), but whose location in FY's diagram is not compatible with such a structure (see red symbols in **Figure 2**). Finally, it is worth mentioning that the anomaly would also probably affect BVO_4, whose structure is unknown (Ref. (9)-p10). Therefore, it is clear that all boron-containing ABO_4 compounds put into question the predictive capability of FY's diagram, both in terms of their structures at ambient pressure and of their pressure-induced phase transitions. For these reasons, the orthoborate subfamily was not allocated in the original FY's diagram (11). Only BPO_4 and $BAsO_4$, two well-known compounds, were allocated in this diagram, assuming they were a phosphate and an arsenate, respectively, and their anomalous pressure-induced phase transitions was barely commented in the work.

The anomaly of BPO_4 and $BAsO_4$ was noted by Bastide (12) who, following Dachille and Roy's initiative (8), classified ABO_4 compounds using the cation and anion sizes as the main criterion. Taking into account the smaller ionic radius (31) of B (0.11 Å) as opposed to those of P (0.17 Å) and As (0.34 Å), Bastide renamed these two compounds PBO_4 and $AsBO_4$ (12). He suggested that the predictive power of FY's diagram could be recovered if the argument used to identify cations *A* and *B* in ABO_4 compounds was size rather than valence. Under this characterization, all anomalies of boron-based compounds could be solved. However, a definitive justification for this change in the chemical nomenclature was still missing.

In this work we resort to the topology of the electron density in order to justify this choice. The big technical improvements in the high pressure experiments have resulted in the ability to accurately resolve many high-pressure solid structures. Simultaneously, the improvement in computational methods and power, has lead to important improvements in their interpretations. The topological analysis of the electron density, the electron density Laplacian and the ELF has lead to numerous advances in the microscopic understanding of crystal properties in the fields of mineralogy and geosciences. Ormeci and Rosner were able to explain the high total energy of the Sb high pressure structure due to the lack of chemical bond between the chain atoms (32). It has also been possible to associate the location of the proton docking sites determined in several silica polymorphs by FTIR studies with the vicinity of the electron lone pairs (33).

Along this contribution, we follow this direction and show show, by means of *ab initio* total-energy calculations and topology, that BPO_4 and $BAsO_4$ are borates, solving an almost a century-old controversy. Therefore, they will be noted as PBO_4 and $AsBO_4$ from now on. Moreover, we provide a mathematical foundation in terms of chemical hardness for the use of a size criterion over valence and also over polyhedral compressibility in ABO_4 compounds. This result has important implications in Solid State Science, where the polyhedral compressibility approach is still widely used. As an example of the usefulness of our approach, a new FY's diagram, where the new borates follow the main trends, is provided. More generally, our approach lays the foundations for the use of Quantum Mechanics calculations as a source of information that can be used to settle arguments, in which common chemical approaches (size, valence, electronegativity, etc.) lead to different answers.

2. Methods

Electronic structure calculations were carried out within the DFT formalism with a plane-wave pseudopotential approach, as implemented in the Vienna *ab initio* simulation package. We used the Perdew-Burke-Ernzerhof generalized gradient approximation (GGA-PBE) for the exchange-correlation functional (34), and the projector augmented wave (PAW) all-electron description of the electron-ion-core interaction (35). Brillouin-zone integrals were approximated using the Monkhorst-Pack method (36), and the energies converged with respect to k-point density (k-point grid spacing of 2π x 0.03 $Å^{-1}$), and to the plane wave kinetic energy cut-off (600 eV).

Identifying the main unit of a solid from its wave function requires obtaining atomic contributions and the bonding pattern. This can be done resorting to the electron density in the framework of the dynamical system theory (37; 38; 39). This approach was developed by Bader and co-workers in what is known as Quantum Theory of Atoms In Molecules (QTAIM) (40).The electron density presents a rich topology with mountains, valleys, plateau zones, and different kinds of critical points (maxima, saddle, ring, and cage points) where $\nabla\rho(r)$ vanishes. Within QTAIM, the first order saddle points are indicative of the bonding between two atoms, which leads to them being called "bond critical points" (bcps). Zero flux surfaces of the $\nabla\rho(r)$ enclose 3D regions or basins that can be associated with atoms (aka. the basins). In the case of crystals, this partition leads to basins that are finite, disjoint, and space filling, which means the addition of all of them over the unit cell recovers its full, so this non-overlapping and filling partition allows to study the very interesting properties of crystalline materials.

Among the achievements of QTAIM, we may outline the identification of the "nature" of functional groups and the transferability of their properties from one system to another. Currently, QTAIM is being used by both theoreticians and experimentalists in fields ranging from solid state physics and X-ray crystallography to drug design and biochemistry. For a good overview of applications, we refer the readers to Ref. (41).

For each structure, the geometry was optimized at several pressures. The pressure-volume data were used to evaluate the corresponding equation of state (EOS) parameters. The equilibrium volume (V_0) is straightforward obtained whereas the bulk modulus (B_0), and its first pressure derivate (B'_0) have been obtained after fitting the theoretical unit cell volume versus pressure data to the analytical Vinet EOS (42). Polyhedral volumes have been obtained with the program VESTA and also adjusted to the Vinet EOS to obtain polyhedral compressibilities. The topological analysis of the electron density in crystals within the QTAIM approach was carried out using the CRITIC code which takes information on the electron density obtained by *ab initio* calculations from CHGCAR files of VASP program (43; 44). Basin volumes (v_i) and charges (q_i) were calculated by integrating the corresponding density operators. We have checked the performance of the partition by checking the recovery of the unit-cell volume.

The concept of chemical hardness, as defined in conceptual DFT is also used in the text. Indeed, the chemical hardness (45) is given by the second derivative of the energy, E, with respect of the number of electrons, N, at constant chemical potential, ν (i.e. at fixed geometry in our case):

$$\eta = \left(\frac{\partial^2 E}{\partial N^2}\right)_{\nu} = E_{gap}$$

In solids, this quantity yields the band gap, E_{gap}. This quantity can be related to atomic compressibility, κ_i, of as follows (46):

$$\kappa_i = \frac{V}{\eta_i N^2} \tag{3}$$

This equation establishes a link between a microscopic parameter-dictating reactivity (i.e. chemical hardness, or η) and the macroscopic resistance of the solid to external pressures.
This is important, because it makes possible to relate compressibility to the shape and size of the atoms. Indeed, it has been demonstrated that a basic relationship between the chemical hardness of an atom - η_i, and its size - r_i, holds as below (47):

$$\eta_i = -\frac{1}{4r_i} \tag{4}$$

Putting Eq. (3) and (4) together, we can see that, in agreement with common chemical knowledge, atomic compressibility is proportional to atomic size ($\kappa_i \propto r_i$); meaning that ions become softer as their radius increases.

3. Results and Discussion

Table 1. Cell parameters for PBO_4 and $AsBO_4$ from our calculations and previous experimental results.[29] Cell parameter a in Å, B_0 in GPa.

	PBO_4					$AsBO_4$				
	a	c/a	x	B_0	B'_0	a	c/a	x	B_0	B'_0
Theory (Ours)	4.433	1.513	0.132	53.7	4.2	5.584	1.499	0.155	49.5	3.7
Experiment	4.339	1.531	0.140	56.0	4.7	4.467	1.526	0.158	49.0	5.0

The high cristobalite structure of PBO_4 ($AsBO_4$) is derived from the ideal tetragonal cristobalite structure by a tilting of the polyhedra (see arrow in **Figure 1**) around the two-fold axes parallel to the c axis (48; 49). This tilting leads to a departure of the c/a axial ratio and the x position of the O atoms - x_O, from their ideal values in the cristobalite structure ($c/a = \sqrt{2}$, $x_O = 0$ – see **Table 1**). Our calculated values of structural parameters for both PBO_4 and $AsBO_4$ under compression are in rather good agreement with previous experimental and theoretical values and allow drawing conclusions on the behaviour under pressure (29) (see **Figures S2-S5**). Noticeably, our theoretical data yield a bulk modulus of 53.7 GPa (49.5 GPa) for PBO_4 ($AsBO_4$), which is in good agreement with the experimental value of 56.0 GPa (49.0 GPa) (29).

Of special interest are the results for x_O, since this parameter is related to the average tilting angle ϕ (29; 48):

$$\phi = \text{arctg}[4x_O] \quad (1)$$

Unlike many ABO_4 compounds, the low-pressure compressibility of the high cristobalite structure of PBO_4 and $AsBO_4$ is not related to polyhedral compression, but rather to the increase of the tilting angle of the constituting polyhedral units (**Figure 3(top)**). This process results in a collapse of the structural gaps of the a-b plane upon pressurization (movie of the compression mechanism available in **S.I.**). In particular, the highly anisotropic c/a compressibility of $AsBO_4$ (**Figure 3(down)**) has been related to the increase of tilting (29). However, our calculations show that the evolution of the tilting is homogenous for both compounds, meaning that it does not explain the different trends in the c/a ratio observed under compression in $AsBO_4$ (they are not observed in PBO_4).

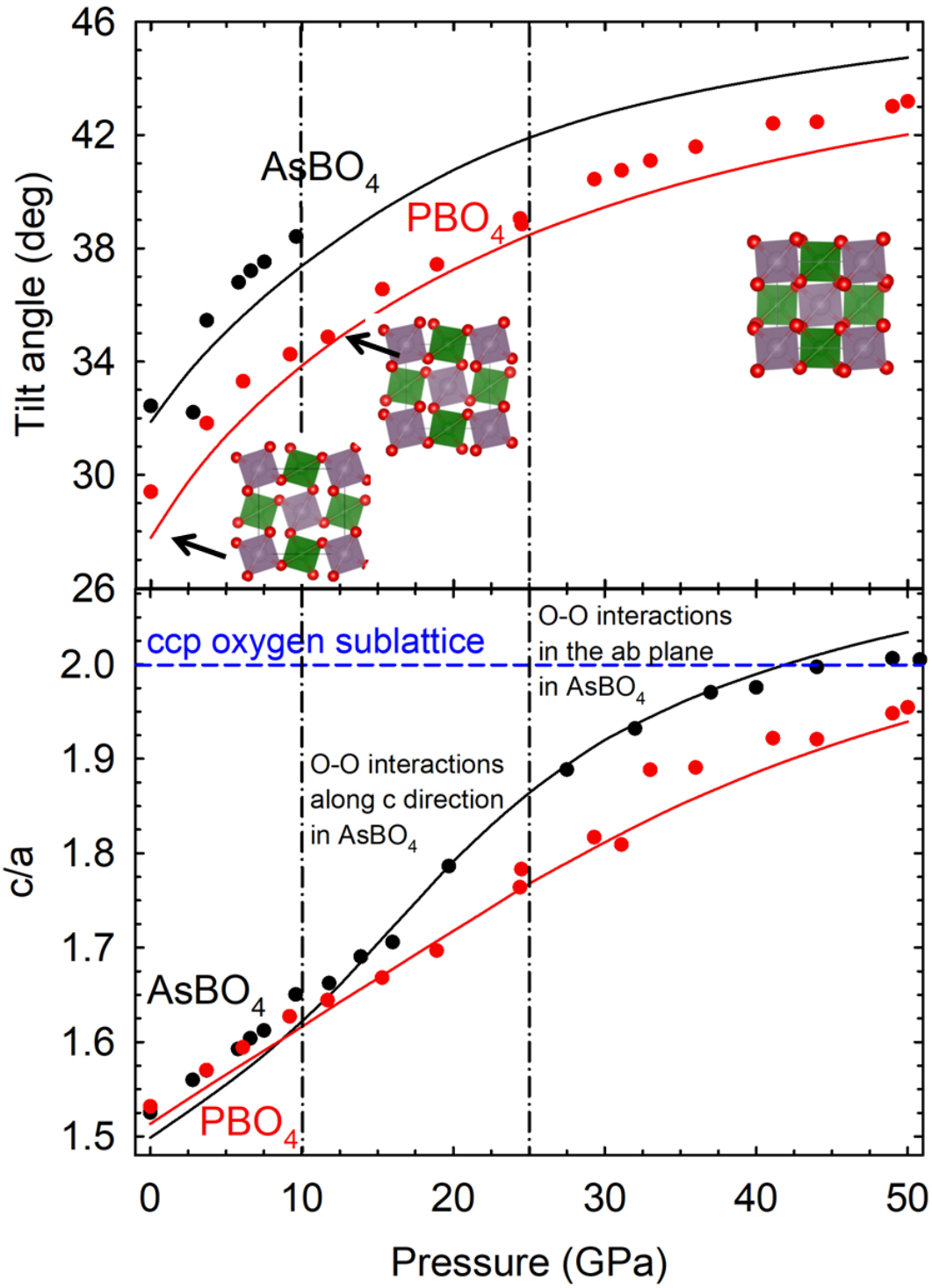

Figure 3. (top) Pressure dependence of polyhedra tilting in PBO_4 (red) and $AsBO_4$ (black) as calculated from Eq. (3). Tilting is shown in the polyhedral representation for some representative pressures. (bottom) Evolution of the *c/a* ratio upon pressurization of PBO_4 (red) and $AsBO_4$ (black). Theoretical dada (lines) are compared to experimental data (symbols) from Ref. 15. Bonding regions are marked with vertical lines and labelled accordingly in the insets.

Following previous studies on the change of polarity of BP under pressure (50), we reviewed the evolution of atomic charges under pressure, but no major changes were found

(**Figure S6**). Instead, our analysis of the electron density showed that tilting results in significant changes in the bonding pattern (see Methods below), which in turn affect the compressibility of the structure. Therefore, the greater size of As relative to P makes the As atom more receptive to these contact changes (see relative atomic volumes in **Table 2**).

Table 2. B_0 (in GPa) for polyhedral units. *X* stands for P/As. Both atomic and void polyhedra are included. T stands for tetrahedron and Oh for octahedral void.

Polyhedron	BO_4	XO_4	Void T1	Void T2	Void T3	Void T4	Void Oh
PBO_4	298.0	648.7	24.20	25.94	107.31	105.30	49.94
$AsBO_4$	251.8	519.0	21.99	26.17	73.24	71.12	45.41

At 0 GPa, common O-As and O-B bonds are observed in **Figure 4a**, where the expected AsO_4 and BO_4 polyhedra are highlighted. Noticeably, new O-O contacts appear between oxygen atoms belonging to different layers at 10 GPa (**Figure 4b**). These contacts occur between the rotating units, such that the *c/a* ratio is only slightly affected. Moreover, new O-O contacts of O atoms in the same *a*-*b* plane are observed above 15 GPa (**Figure 4c**) and again at 22GPa (**Figure 4d**). From a chemical point of view, the new bonds correspond to an O^{2-} polymerization. These O links hinder the tilting, thus explaining the anisotropic behavior of $AsBO_4$. These new set of bonds in turn decrease the compressibility of *c*, leading to a plateau in the *c/a* plot. In summary, the analysis of the electron density permits the explanation of the anisotropic behavior of the high cristobalite structure of $AsBO_4$ as the result of the polymerization of oxygen atoms upon pressurization.

We can also use the information obtained from the electron density to resolve the controversy on the nomenclature of PBO_4 and $AsBO_4$. As commented above, FY's diagram is a good structure field map for describing and predicting the behavior of ABO_4 compounds, except in the case of boron-based compounds (see **Figure 2**). The latter constitute a rare case, in which valence and size give different answers for the designation of *A* and *B* cations; in other words, the choice of the main polyatomic BO_4 unit in these materials becomes crucial. We argue that following Bastide's initiative (12), size constitutes a better criterion than valence. In such a case, BPO_4 and $BAsO_4$ with $k<1$ will become PBO_4 and $AsBO_4$ with $k > 1$, and their phase transition will follow the south-east rule, like all other ABO_4 compounds in FY's diagram (compare **Figures 5(top)-(down)**).

The south-east rule in FY's diagram implies that cation *A* compresses faster than cation *B*. It is the effect of this rule on *k* that accounts for the failure of the boron compounds to reproduce the general behavior. Hence, the crucial factor in the classification of these compounds is the compression rate of *A* and *B* cations. Historically, this was checked by means of the polyhedral approach explained above. However, in the case of compounds such as PBO_4 and $AsBO_4$, whose main compression mechanism is tilting, this approach is inadequate, meaning that the compressibility of these compounds is not related to the compressibility of atomic polyhedra, but to the compression of the voids between them (**Figure 3**). In order to prove it, we calculated the evolution of the tetrahedral (T) and Octahedral (Oh) voids in the high cristobalite structure upon pressurization (see **Table 2** and **Figure S7**). It can be seen that it is precisely these void units, not attributable to any given atom within the polyhedral approach, which are mainly responsible for the compression of the high cristobalite structure of both PBO_4 and $AsBO_4$. Note that the compressibility of the voids in PBO_4 ($AsBO_4$) is more similar to that of the bulk than those of the BO_4 and PO_4 (AsO_4) units, whose relative volume decrease is less than 10%, up to 50 GPa. Hence, we can see that the historical polyhedral approach is not valid for rationalizing the behavior of structures with voids, like the high cristobalite structures of PBO_4 and $AsBO_4$.

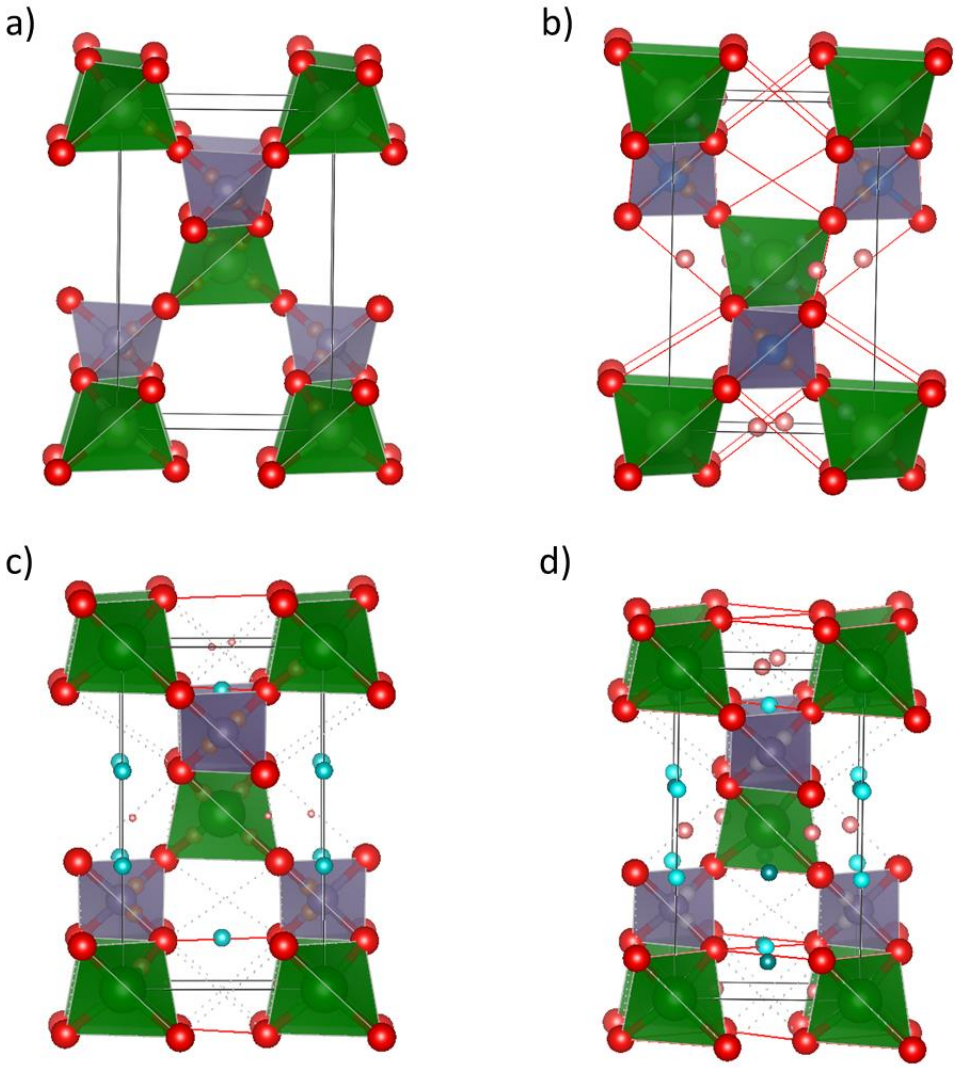

Figure 4. Evolution of bond critical points (bcps) in compressed $AsBO_4$ at 0 GPa (a), 10 GPa (b), 15 GPa (c), and 22 GPa (d). Oxygen in red, As in green, and B in purple. Bcps are represented with small spheres: O-As and O-B bonds at 0 GPa (in orange), O-O bonds at 10 GPa (pink), interlayer bonds at 15 GPa (blue), and 22 GPa (green). Polyhedra have been colored in blue (BO_4) and green (AsO_4) at 0 GPa to facilitate differentiation of As-O and B-O bonds at room pressure.

In order to generalize the size concept in FY's and Bastide's diagrams, a definition of atomic volumes without voids is needed. Such definition is provided by the atomic partition introduced by the topological analysis of the electron density within QTAIM. This approach associates the region around each atom to each nucleus, just as a mountain is represented by its summit. This provides a finite basin volume Ω_i to each atom i, which results in no voids left in the structure because the sum of all Ω_i results in the total unit cell volume. Using this definition of atomic volumes, the macroscopic compressibility of the crystal can be expressed as a sum of atomic contributions, as follows:

$$\kappa = -\frac{1}{V}\frac{\partial V}{\partial P} = \sum f_i \kappa_i \quad (2)$$

where κ_i defines the atomic compressibility, while $f_i = V_i/V$ is the fractional occupation volume of the i-th atom (of volume V_i) in the unit cell of volume V (51; 52). Under this representation, not only basin volumes and charge populations are additive, but compressibility as well. It should be noted that this definition of atomic compressibility is

applicable to other non-overlapping partitions that fill the whole volume (e.g. Voronoi).

Table 3. Atomic bulk moduli B_{0i} (in GPa) as determined from QTAIM.

	PBO_4		$AsBO_4$	
Atom i	B_{0i}	f_i	B_{0i}	f_i
O	48.0	0.785	42.0	0.862
P/As	117.5	0.172	98.5	0.118
B	150.9	0.043	128.3	0.019

The evolution upon compression of the volume of the QTAIM atomic basins Ω_i for P (As), B, and O in the high cristobalite structure of PBO_4 ($AsBO_4$) is shown in **Figure S8**. Furthermore, atomic bulk moduli have been calculated following Eq. (2) from a Vinet fit, leading to the data collected in **Table 3**. It can be observed that the largest compressibility (largest slope) corresponds to the O atom, while the smallest compressibility (smallest slope) corresponds to the B atom. Consequently, electron-density derived volumes within QTAIM clearly indicate that the compressibility of the B atom is much smaller than that of the P and As atoms, thus suggesting that the boron atom must be the *B* atom in boron-containing ABO_4 compounds. This result also points to the relevance of electron density studies in Solid State Science, as already highlighted in the growing field of Quantum Crystallography (53).

In summary, the QTAIM approach yields the ability to discern the hardest atom, and as a result, find the main polyatomic unit. It does, however, have the disadvantage of requiring the calculation of the EOS for every atomic contribution, which can be cumbersome. Fortunately, we can design several layers of approximations to circumvent it. Looking back at Eq. (2), the contribution of an ion to the total compressibility will depend on its relative volume in the cell - f_i, but also on its compressibility - κ_i. It has been shown that hydrostatic compressibility of an atom i is inversely proportional to it hardness, η_i (see Methods for greater details) (46):

$$\kappa_i = \frac{V}{\eta_i N^2} \tag{3}$$

where N represents the number of atoms in the unit cell of volume V.
This equation establishes a link between a microscopic parameter-dictating reactivity (i.e. chemical hardness, or η) and the resistance of the solid to external pressures. This is important, because it makes it possible to relate compressibility to the shape and size of the atoms. Indeed, it has been demonstrated that hardness is inversely proportional to the atomic size (47). Putting these concepts together (see Methods for a complete derivation), we can see that, in agreement with common chemical knowledge, atomic compressibility is proportional to atomic size ($\kappa_i \propto r_i$). In other words, according to common acceptance, ions become softer as their radius increases. **Figure S9** shows that this relationship holds for all the different ions in PBO_4 and $AsBO_4$. Although we have used radii derived from the solid within QTAIM (assuming a spherical approximation, $r_{QTAIM}=3V^{1/3}/(4\pi)$), the relationship also holds for Shannon ionic radii. In summary, this method provides a working horse approximation in order to *a priori* determine the hard ions in a crystal, and hence the polyanion complex. Furthermore, we have provided the physical foundation for the prevalence of size over valence that should dictate the attribution of *A* and *B* cations in ABO_4 compounds. Consequently, the nomenclature of these compounds should be guided by size, simultaneously restoring the predictive character of structure field maps.

We want to highlight that all the results reported here for PBO_4 and $AsBO_4$ have several consequences from the chemical point of view. First and foremost, the BO_4 units (including their corresponding structural voids) are the less compressible ones; therefore, they can be considered as the main structural polyatomic units of these two pseudo-binary compounds. Second, these two compounds should be considered borates and not a phosphate and an arsenate, respectively, as was previously assumed. In other words, the notation according to their properties should rather be PBO_4 and $AsBO_4$, instead of BPO_4 and $BAsO_4$, respectively.

From the high pressure point of view, the demonstrated proportionality of the bulk

moduli to size (Eq. (3) - (5)) confirms the use of ionic radii as a good approximation for classifying polyatomic anions and ensuring a coherent nomenclature in ambiguous cases. We propose the use of the larger ionic radius when choosing the *A* cation in ABO_4 compounds within FY's diagram, as it is done in Bastide's diagram. Hence, all ABO_4 compounds in FY's diagram must have k > 1. This would lead to the re-allocation of both PBO_4 and $AsBO_4$ in the revised FY's diagram (**Figure 5 (down)**), and the use of the "south-east" rule for understanding pressure-induced phase transitions in all ABO_4 compounds.

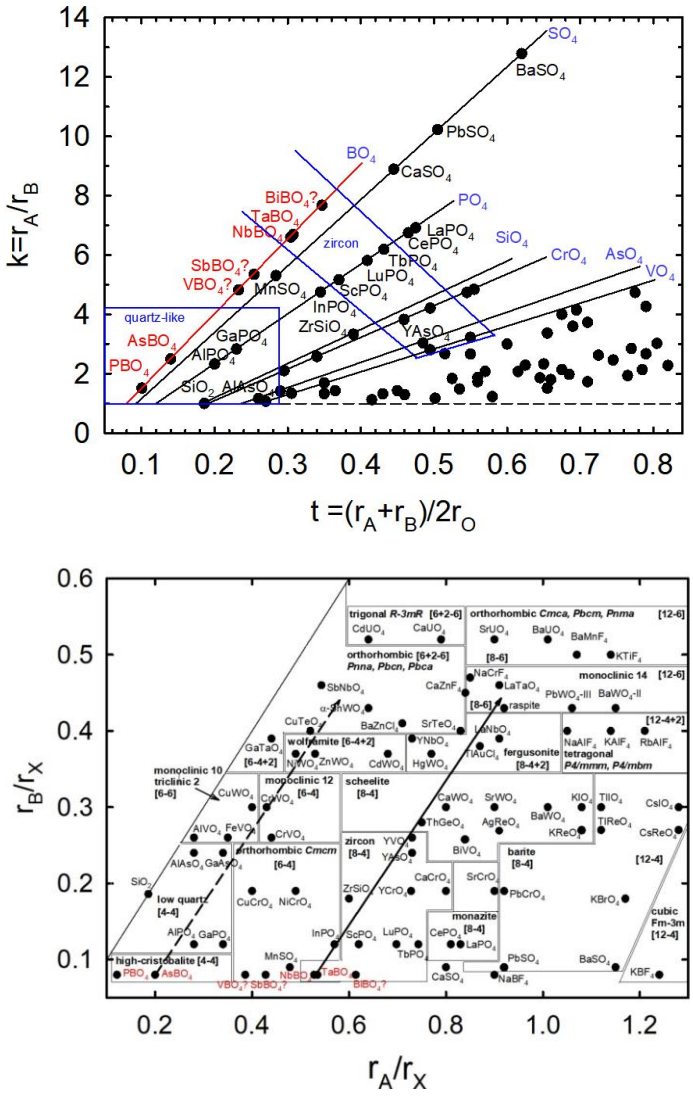

Figure 5. (top) Bastide's diagram for ABO_4 compounds. The whole family of borates is indicated in red. (bottom) Corrected FY's diagram with PBO_4 and $AsBO_4$ re-allocated by considering that both are borates. The family of borates is highlighted in red color.

Most importantly, this redefinition of FY's diagram reinforces its predictive power even for unknown phases. This ensures a low-cost understanding of new phases and their transformations, which we can now test. In particular, if the very rare zircon-type minerals schiavinatoite ($NbBO_4$) and behierite ($TaBO_4$) are included as borates, the orthoborate subfamily is further enlarged. According to the corrected FY's diagram, as well as Bastide's diagram, $NbBO_4$ and $TaBO_4$ should crystallize in the zircon structure and transform under pressure to either the scheelite or the monazite phase. Testing this hypothesis with our

calculations on the three phases, we can conclude that, at zero pressure, the zircon type structure is indeed more stable than the scheelite and monazite phases. Moreover, we predict a pressure-induced phase transition from the zircon structure towards the scheelite phase (see **Figure S10**) at 47.5 GPa (52.0 GPa) for $NbBO_4$ ($TaBO_4$). It is important to remark that the orthoborate family of ABO_4 compounds is the only one featuring the *A* cation with a greater valence (+5) than the *B* cation (+3).

In addition, the redefinition of the chemical nomenclature of PBO_4 and $AsBO_4$ creates the opportunity for exploring interesting new avenues. It opens the door for the possible synthesis of other ABO_4 compounds with *A* atoms from the 5B group (Sb, Bi). According to the corrected FY's and Bastide's diagrams, $SbBO_4$ and $BiBO_4$ should crystallize in the compact orthorhombic *Cmcm,* and tetragonal zircon-type structures, respectively, and the yet unknown structure of VBO_4 could also belong to the *Cmcm* symmetry (see **Fig. 5**).

4. Conclusions

We have shown, by means of an analysis of the electron density provided by Quantum Mechanics calculations, that the chemical nomenclature of pseudo-binary compounds, like the ABO_4 ones, is not yet a solved issue. Until now, the identification of polyatomic anions relied on chemical knowledge and in most cases, the analysis of the valence and the size of the atoms provided a mutually coherent answer. What we have shown instead is that, in boron-containing ABO_4 compounds, like PBO_4 and $AsBO_4$, this is not the case. Boron (χ=2.04, Pauling scale) has a similar electronegativity to that of phosphorous (χ=2.19) and arsenic (χ=2.18). Phosphorous and arsenic hold a higher valence (+5) than boron (+3), which usually leads to harder anions. However, the small size of boron (r_B= 0.11 Å, r_P=0.17 Å and r_{As}=0.34 Å) leads to an important competition. In fact, the chemical hardness of these ions at their formal charge is largely more important for B^{3+} (η_{B3+}= 221 eV, η_{P5+}=155 eV and η_{As5+}=65 eV) despite its smaller valence. Consequently, our calculations show that boron must be the *B* cation in boron-containing ABO_4 compounds.

Our results are of important implications for general Chemistry and Solid State Sciences. The first consequence is that the two compounds need to be renamed as phosphorous borate (PBO_4) and arsenic borate ($AsBO_4$) - a nomenclature in agreement with their properties. We must emphasize that this result prompts for the revision of the nomenclature of borophosphates, which perhaps should be renamed as phosphoroborates (54). Secondly, it would mean that the general FY's diagram of ABO_4 compounds should be reformulated in terms of size instead of valence, in order to be able to welcome novel structures while keeping its predictive power. In this way, both FY's and Bastide's diagrams for ABO_4 compounds are defined on the same roots. Thirdly, the new borates PBO_4 and $AsBO_4$ form - together with $NbBO_4$, $TaBO_4$, and the poorly known VBO_4 - the orthoborate subfamily; i.e., the only ABO_4 compounds with the *A* cations having a valence higher than +4; this could also mean that zircon-type borates could be the most uncompressible ABO_4 compounds, due to the well-known relationship between the bulk modulus and the formal charge of the *A* cation in zircon-type compounds (13; 26). Fourthly, the existence of PBO_4 and $AsBO_4$ opens the door for the synthesis of new members of the borate family with *A* cations of a +5 valence, such as the yet unknown $SbBO_4$ and $BiBO_4$ compounds.

Finally, from a more general perspective we can draw two main conclusions. With respect to Chemistry, the nomenclature of compounds is still an open topic and Quantum Mechanics calculations, together with electron density analysis, can help us to improve it. More specifically, this is another example that QTAIM is a powerful tool for understanding crystal properties. As an example, Zhang et al were recently able to explain the isotropic thermoelectric properties of Mg_3Sb_2 from the bonding network (55). In our case, we have highlighted the need to resort to QTAIM for the identification of the main polyanions in ternary systems, which still remained defined in terms of chemical intuition. Resorting to a general rationalization in terms of properties, these ambiguities can be solved when

characteristics such as valence or size do not run in the same direction. In relation to Physics, the historical polyhedral approach has been shown not to be valid for rationalizing the behavior of structures with voids under compression, like the high crystobalite structure. In these cases, the analysis of electron density can facilitate the definition of extended concepts. As an example, Rahm et al have recently redefined electronegativity leading to a scale similar to Allen's (56). Here, we have shown that the use of QTAIM atomic volumes enables to recover the predicting capability of structure field maps.

Acknowledgements - We especially acknowledge the availability of experimental data of PBO4 and AsBO4 kindly provided by J. Haines, and the discussions with Dr. J.A. Sans. This research was partially supported by Spanish MINECO (MAT2015-71070-REDC and MAT2016-75586-C4-2-P) and Generalitat Valenciana (PROMETEO/2018/123). JCG thanks CALSIMLAB under the public grant ANR-11-LABX-0037-01, overseen by the French National Research Agency (ANR) as part of the Investissements d'Avenir program (reference: ANR-11-IDEX-0004-02).

Supporting Information

Film for the PBO_4 compression. ABO_4 subfamilies. Theoretical and computational details. Figures: S1) Evolution of BO_4 and AO_4 (A=P,As) polyhedral volumes with pressure. S2) Pressure dependence of experimental and theoretical cell parameters; O atomic parameters in PBO_4. S3) Pressure dependence of experimental and theoretical cell parameters; and O atomic parameters in $AsBO_4$. S4) Pressure dependence of experimental and theoretical unit cell volume in PBO_4 and $AsBO_4$. S5) Pressure dependence of the enthalpy difference per formula unit between the berlinite structure with respect to the high cristobalite structure for PBO_4 and $AsBO_4$. S6) Pressure dependence of QTAIM charges in PBO_4 and $AsBO_4$: a) Total atomic charges, b) Absolute change of the atomic charges with respect to 0 GPa, and c) Relative change of the atomic charges with respect to 0 GPa. S7) Pressure dependence of QTAIM void volumes at tetrahedral and octahedral voids in PBO_4 and $AsBO_4$. S8) Pressure dependence of QTAIM atomic basin relative volumes in PBO_4 and $AsBO_4$. S9) Pressure dependence of the atomic bulk modulus, B_{0i}, as a function of $1/r_i$ in PBO_4 and $AsBO_4$. S10) Pressure dependence of the enthalpy difference per formula unit between the scheelite and monazite structures with respect to the zircon structure in $NbBO_4$ and $TaBO_4$.

References

1. Pauling, L. (1929), J. Am. Chem. Soc., **51**, 1010–1026.

2. Pauling, L. (1960) The nature of the chemical bond and the structure of molecules and crystals; an introduction to modern structural chemistry. [ed.] 543-562 Cornell University Press. 3rd. Ithaca (NY) : s.n.

3. Nomenclature of inorganic solids. Definitive rules (1970) London : International Union of Pure and Applied Chemistry.
4. Li, H. ; Zhou, S. ; Zhang, S. (2007) J. Solid State Chem., **180**, 599-605.
5. Scott, H.P.; Williams, Q.; Knittle, E. (2001) Phys. Rev. Lett., **88**, 015506 .
6. Liu, L.G. (1982) Earth and Planetary Science Letters, **57**, 110-116.
7. Müller, O.; Roy, R. (1973) Z. Kristall., **138**, 237 - 253.
8. Dachille, F.; Roy, R. (1959) Z. Kristall., **111**, 451 – 461.
9. Stubican, V.V.; Roy, R. (1962) Z. Kristall., **119**, 90 – 97.
10. Vorres, K.S. (1962) J. Chem. Edu., **39**, 566.
11. Fukunaga, O. ; Yamaoka, S. (1979) Phys. Chem. Minerals, **5**, 167-177.
12. Bastide, J. P. (1987) J. Solid State Chem., **71**, 115-120.
13. Errandonea, D.; Manjón, F.J. (2008) Prog. Mat. Sci., **53**, 711-773.
14. Lashin, V.E.; Khritokhin, N.A.; Andreev, O.V. (2012) Russ. J. Inorg. Chem., **57**, 1584–1587.
15. Depero, L.E.; Sangaletti, L. (1997) J. Solid State Chem., **129**, 82-91.
16. Zaslavskij, A.I.; Zvincuk, R.A. (1953) Dokl. Aknd. Nauk SSSR, **90**, 781.
17. Mrose, M.E.; Rose, W.J. (1961) Am. Min. Soc. Prog. A, **111**.
18. Bayer, G. (1972) J. Less-common Metals, 26, 255-262.
19. Range, K.J.; Wildenauer, M.; Heyns, A.M. (1988) Angew. Chem Int. Ed. Engl , **27**, 969-971.
20. Gramaccioli, C.M. (2000) Rend. Fis. Acc. Lincei, **11**, 197-199.
21. Demartin, F.; Diella, V.; Gramaccioli, C.M. ; Pezzotta, F. (2001) Eur. J. Mineral, **13**, 159-165.
22. Blase, G.; Van den Heuvel, G.P.M. (1973) Phys. Stat. Sol. A, **19**, 111-117.
23. Gramaccioli, C.M. (2000) Rendiconti Lincei, **11**, 197-199.
24. Schulze G. E. (1933) Naturwissenschaften **21**, 562–562
25. Machatschki F. (1936) Z. Kristall., **94**, 222 .
26. Brill, R.; de Bretteville, A.P. (1955) Acta Cryst., **8**, 567-570.
27.Hazen, R.M; Finger, L.W.; Mariathasan, J.W.E. (1985) J. Phys. Chem. Solids, **46**, 253-263.
28.Hazen, R.M.; Finger, L.W. (1979) J. Geophys. Res., **84**, 6723.
29. Haines, J.;Chateau, C.; Léger, J.M ; Bogicevic, C. ; Hull, S. ; Klug, D.D. ; Tse, J.S. (2003) Phys. Rev. Lett., **91**, 015503 .
30. Dachille, F.; Glasser, L.S.D. (1959) Acta Cryst., **12**, 820-821.
31. Shannon, R.D. (1976) Acta Cryst. A, A**32**, 751-767.
32.Ormeci, A.; Rosner, H. (2004) Z. Kristallogr., **219**, 370–375.
33. Gibbs, G. V.; Cox, D. F.; Boisen Jr., M. B.; Downs, R. T.; Ross, N. L. (2003) Phys. Chem. Minerals, 30, 305–316.
34. Perdew, J.P.; Burke, K.; Ernzerhof, M. (1996) Phys. Rev. Lett., **77**, 3865-3868.
35.Kresse, G.; Joubert, D. (1999), Phys. Rev. B, **59**, 1758.
36.Monkhorst, H.J.; Pack, J.D. (1976) Phys. Rev. B, 13, 5188.
37.Bader, R. F. W. Encyclopedia of Computational Chemistry. [ed.] N. L. Alinger, T. Clark, J. Gasteiger, P. A. Kollman, H. F. Schaefer III, P. R. Schreiner P. von R. Schleyer. s.l. (1998) Wiley: Chichester.

38.Bader, R.F.W. (1994) Phys. Rev. B, **49**, 13348.
39.Abraham, R.H.; Marsden, J.E. Foundations of Mechanics. Reading (1994) Addison Wesley.
40.Bader, R. F. W. Atoms in Molecules, A Quantum Theory. (1990) Oxford : Clarendon.
41. Boyd, R.J.; Matta, C.F Eds. The Quantum Theory of Atoms in Molecules. From Solid State to DNA and Drug Design. (2007) Weinheim : Wiley-VCH.
42. Vinet, P.; Ferrante, J.; Smith, J. R.; Rose, J.H. (1986) J. Phys. C: Solid State Phys. L, **19**, 467 .
43. Otero-de-la-Roza, A.; Blanco, M. A.; Martín Pendás, A.; Luaña, V. (2009) Comput. Phys. Commun., **180**, 157.
44. Otero-de-la-Roza, A. ; Contreras-Garcia, J.; Johnson, E.R. (2012) Phys. Chem. Chem. Phys., **14**, 12165 .
45. Geerlings, P. ; De Proft, F.; Langenaeker, W. (2003) Chem. Rev., **103**, 1793-1874.
46.Yang, W.; Parr, R.G.; Uytterhoeven, L. (1987) Physics and Chemistry of Minerals, **15**, 191-195.
47.Gásquez, J.L.; Ortiz, E. (1984) J. Chem. Phys., **81**, 2741.
48. O'Keefe, M.; Hyde, B.G. (1976) Acta Crystallogr. Sect. B, **32**, 2923-2936 .
49. Léger, J.M. ; Haines, J.; Chateau, C. ; Bocquillon, G. ; Schmidt, M.W. ; Hull, S. ; Gorelli, F. ; Le Sauze, A. ; Marchand, R. (2001) Phys. Chem. Miner., **28**, 388-398.
50. Mori-Sanchez, P.; Martin Pendas, A.; Luaña, V. (2001) Phys. Rev. B, **63**, 125103 .
51. Martín Pendás, A.; Costales, A.; Blanco, M.A. ; Recio, J.M.; Luaña, V. (2000) Phys. Rev. B., **62**, 13970 .
52.Recio, J.M.; Franco, R.; Martín Pendás, A.; Blanco, M.A.; Pueyo, L.; Pandey, R. (2001) Phys. Rev. B, **63**, 184101 .
53. Genoni, A.; Bučinský, L.; Claiser, N. ; Contreras-García, J. ; Dittrich, B.; Dominiak, P.M. ; Espinosa, E.; Gatti, C. ; Giannozzi, P. et al. (2018) Chem. Eur. J., **24**, 10881-10905.
54. Kniep, R. ; Gozel, G. ; Eisenmann, B. ; Rohr, C. ; Asbrand, M.; Kizilyalli, M. (1994) Angew. Chem. Int. Ed. Engl., **33**, 749-751.
55. Zhang, J.; Song, L.; Sist, M.; Tolborg, K; Iversen, B.B. (2018) Nature Communications, **9**, 4716.
56. Rahm, M.; Zehn, T.; Hoffmann, R. (2019) J. Am. Chem. Soc., **141**, 342-351.